[redacted]

Copy 44
RM SL55E02

NACA

RESEARCH MEMORANDUM

for the

Bureau of Aeronautics, Department of the Navy

WIND-TUNNEL INVESTIGATION AT LOW SPEED OF THE ROLLING STABILITY DERIVATIVES OF A 1/10-SCALE MODEL OF THE GRUMMAN F9F-9 AIRPLANE

TED NO. NACA AD 3109

By Walter D. Wolhart and David F. Thomas, Jr.

Langley Aeronautical Laboratory
Langley Field, Va.

NATIONAL ADVISORY COMMITTEE FOR AERONAUTICS

WASHINGTON

[redacted]

NACA RM SL55E02

NATIONAL ADVISORY COMMITTEE FOR AERONAUTICS

RESEARCH MEMORANDUM

for the

Bureau of Aeronautics, Department of the Navy

WIND-TUNNEL INVESTIGATION AT LOW SPEED OF THE ROLLING STABILITY DERIVATIVES OF A 1/10-SCALE MODEL OF THE GRUMMAN F9F-9 AIRPLANE

TED NO. NACA AD 3109

By Walter D. Wolhart and David F. Thomas, Jr.

SUMMARY

An experimental investigation has been made in the Langley stability tunnel to determine the low-speed rolling stability derivatives of a 1/10-scale model of the Grumman F9F-9 airplane. Tests were made to determine the tail contributions as well as the effect of duct-entrance fairing plugs, slats, flaps, flaperons, and landing gear. The effect of sideslipping the model -10° was determined for one of the clean configurations. These data are presented without analysis in order to expedite distribution of the paper.

INTRODUCTION

Previous investigations have indicated that reliable prediction of dynamic flight characteristics over a wide angle-of-attack range requires more accurate estimates of the various aerodynamic parameters than is possible with the use of available procedures. (See refs. 1 and 2, for example.)

The purpose of the present investigation was to determine the rolling stability derivatives of various clean and landing configurations of a 1/10-scale model of the Grumman F9F-9 airplane. These tests were made at the request of the Bureau of Aeronautics, Department of the Navy, to aid in the development of the Grumman F9F-9 airplane. The results of a previous investigation to determine the static, yawing, and pitching stability characteristics of the same model are given in reference 3.

SYMBOLS

The data presented herein are in the form of standard NACA coefficients of forces and moments which are referred to the stability system of axes shown in figure 1. All coefficients are based on the basic-wing area of 2.502 square feet rather than on the total area of 2.548 square feet for the basic wing and the leading-edge extension. The positive direction of forces, moments, and angular displacements is shown in figure 1. The coefficients and symbols are defined as follows:

L	lift, lb
D	drag, lb
Y	side force, lb
M	pitching moment, ft-lb
L'	rolling moment, ft-lb
N	yawing moment, ft-lb
b	span, ft
s	area, sq ft
q	free-stream dynamic pressure, $\frac{\rho V^2}{2}$, lb/sq ft
V	free-stream velocity, ft/sec
ρ	mass density of air, slugs/cu ft
α	angle of attack of fuselage reference line, deg
θ	angle of pitch, deg
γ	flight-path angle, deg
ϕ	angle of roll about wind axis, deg
β	angle of sideslip, deg

ψ angle of yaw, deg

C_Y lateral-force coefficient, Y/qS_w

C_l rolling-moment coefficient, L'/qS_wb_w

C_n yawing-moment coefficient, N/qS_wb_w

$\frac{pb}{2V}$ flight-path helix angle, radians

p rolling angular velocity (measured with respect to wind axes), $d\phi/dt$

$$C_{Y_p} = \frac{\partial C_Y}{\partial \frac{pb}{2V}}$$

$$C_{l_p} = \frac{\partial C_l}{\partial \frac{pb}{2V}}$$

$$C_{n_p} = \frac{\partial C_n}{\partial \frac{pb}{2V}}$$

Subscript:

w wing

Model-Component Designations

W wing

B fuselage

V vertical tail

H horizontal tail (used with subscripts 0 or -10 to denote horizontal incidence, in degrees)

Z wing fences

P duct-entrance fairing plugs

G landing gear extended

F flaps deflected (used with subscript 30 to denote flap deflection, in degrees, with respect to wing chord line)

s slats extended

δ flaperon deflected (used with superscripts 5, 25, or 55 to denote flaperon deflection, in degrees, with respect to local upper surface of wing)

Subscripts:

L left

R right

APPARATUS AND MODEL

The tests of the present investigation were made in the 6-foot-diameter rolling-flow test section of the Langley stability tunnel in which rolling flight is simulated by rolling the airstream about a stationary model (ref. 4). Forces and moments on the model were obtained with the model mounted on a single strut support which in turn was fastened to a conventional six-component balance system.

The model used in this investigation was a 1/10-scale model of the Grumman F9F-9 airplane and was supplied to the National Advisory Committee for Aeronautics by the Grumman Aircraft Engineering Corp. Pertinent geometric characteristics of the model are given in figure 2 and table I. Lateral control on this airplane is provided by flap-type spoiler controls called flaperons (see fig. 2(b)). The left and right flaperons are deflected independently of one another to give left and right rolls, respectively. A symmetrical flaperon deflection of 5°, designated δ_{LR}^{5}, corresponds to the neutral flaperon position for all flaps-extended configurations. Photographs of the model are presented in figures 3 and 4. No provisions were made for internal flow; however, removable duct-entrance fairing plugs were provided so that any interference effects from this area could be determined.

TESTS

All the tests were made at a dynamic pressure of 24.9 pounds per square foot which corresponds to a Mach number of about 0.13 and a Reynolds number of 0.756×10^6 based on the wing mean aerodynamic chord of 0.82 foot. The angle-of-attack range for all tests was from approximately -4° to 20°. The rolling derivatives were determined from tests made at values of $pb/2V$ of -0.074, -0.048, -0.028, 0, 0.008, 0.033, and 0.064. Most of the tests were made at $\beta = 0^\circ$; however, one configuration was tested at $\beta = -10^\circ$.

CORRECTIONS

Approximate corrections for jet-boundary effects were applied to the angle of attack by the methods of reference 5. The dynamic pressure has been corrected for the effects of blockage by the methods of reference 6. These data have not been corrected for the effect of the support strut or for the effective pitching velocity which exists when the model is rolled at an angle of sideslip.

PRESENTATION OF RESULTS

The results of this investigation are presented in figures 5 to 10. For convenience in locating desired information, a summary of the model configurations investigated as well as the figures that give data for these configurations is given in table II. These data are presented without analysis in order to expedite distribution of the paper.

Langley Aeronautical Laboratory,
National Advisory Committee for Aeronautics,
Langley Field, Va., April 18, 1955.

Walter D. Wolhart
Walter D. Wolhart
Aeronautical Research Scientist

David F. Thomas, Jr.
David F. Thomas, Jr.
Aeronautical Research Scientist

Approved: Thomas A. Harris
Thomas A. Harris
Chief of Stability Research Division

sam

REFERENCES

1. Jaquet, Byron M., and Fletcher, H. S.: Lateral Oscillatory Characteristics of the Republic F-91 Airplane Calculated by Using Low-Speed Experimental Static and Rotary Derivatives. NACA RM L53G01, 1953.

2. Campbell, John P., and McKinney, Marion O.: Summary of Methods for Calculating Dynamic Lateral Stability and Response and for Estimating Lateral Stability Derivatives. NACA Rep. 1098, 1952. (Supersedes NACA TN 2409.)

3. Wolhart, Walter D., and Thomas, David F., Jr.: Wind-Tunnel Investigation at Low Speed of the Yawing, Pitching, and Static Stability Characteristics of a 1/10-Scale Model of the Grumman F9F-9 Airplane - TED No. NACA AD 3109. NACA RM SL55D25, Bur. Aero., 1955.

4. MacLachlan, Robert, and Letko, William: Correlation of Two Experimental Methods of Determining the Rolling Characteristics of Unswept Wings. NACA TN 1309, 1947.

5. Silverstein, Abe, and White, James A.: Wind-Tunnel Interference With Particular Reference to Off-Center Positions of the Wing and to the Downwash at the Tail. NACA Rep. 547, 1936.

6. Herriot, John G.: Blockage Corrections for Three-Dimensional-Flow Closed-Throat Wind Tunnels, With Consideration of the Effect of Compressibility. NACA Rep. 995, 1950. (Supersedes NACA RM A7B28.)

TABLE I

GEOMETRIC CHARACTERISTICS OF 1/10-SCALE MODEL OF THE GRUMMAN F9F-9 AIRPLANE

Wing (does not include leading-edge extension):	
Aspect ratio	4.00
Taper ratio	0.50
Quarter-chord sweep angle, deg	35.00
Dihedral angle, deg	-2.50
Airfoil section at root	Modified NACA 65A006
Airfoil section at tip	Modified NACA 65A004
Root chord, ft	1.053
Tip chord, ft	0.526
Area, sq ft	2.502
Span, ft	3.165
Mean aerodynamic chord, ft	0.820
Horizontal tail:	
Aspect ratio	3.50
Taper ratio	0.40
Quarter-chord sweep angle, deg	35.00
Airfoil section at root	NACA 65A006
Airfoil section at tip	NACA 65A004
Root chord (on fuselage reference line), ft	0.619
Tip chord, ft	0.248
Area, sq ft	0.655
Span, ft	1.519
Mean aerodynamic chord, ft	0.460
Tail length (distance from center of gravity to $\bar{c}/4$ of tail), ft	1.260
Vertical tail:	
Aspect ratio	1.50
Taper ratio	0.18
Quarter-chord sweep angle, deg	44.45
Airfoil section at root	NACA 65A006
Airfoil section at tip	NACA 65A006
Root chord (measured 2.70 in. above fuselage reference line), ft	0.875
Tip chord, ft	0.155
Area, sq ft	0.479
Span (measured from 2.70 in. above fuselage reference line), ft	0.775
Tail length (distance from center of gravity to $\bar{c}/4$ of tail), ft	1.234

TABLE II

SUMMARY OF MODEL CONFIGURATIONS TESTED AND DATA PRESENTED

Model configuration	Data presented (C_{Y_p}, C_{n_p}, and C_{l_p} plotted against α)	Figure
WBZP $WBZPVH_0$ $WBZVH_0$	Effect of horizontal and vertical tails and effect of duct-entrance fairing plugs on clean configuration	5
$WBZPF_{30}S\delta_{LR}^{5}$ $WBZPVH_{-10}F_{30}S\delta_{LR}^{5}$ $WBZPVH_{-10}F_{30}S\delta_{LR}^{5}G$	Effect of horizontal and vertical tails and effect of landing gear on landing configuration	6
$WBZPVH_0$ $WBZPVH_0\delta_L^{25}$ $WBZPVH_0\delta_L^{55}$	Effect of flaperon deflection on clean configuration	7
$WBZPVH_{-10}F_{30}S\delta_{LR}^{5}G$ $WBZPVH_{-10}F_{30}S\delta_L^{25}\delta_R^{5}G$ $WBZPVH_{-10}F_{30}S\delta_L^{55}\delta_R^{5}G$	Effect of flaperon deflection on landing configuration	8
$WBZPF_{30}S\delta_L^{55}\delta_R^{5}G$ $WBZPVH_{-10}F_{30}S\delta_L^{55}\delta_R^{5}G$	Effect of horizontal and vertical tails on landing configuration	9
$WBZP\delta_L^{55}$ $WBZPVH_0\delta_L^{55}$ $WBZPVH_0\delta_L^{55}$, $\beta = -10$	Effect of horizontal and vertical tails and effect of sideslip angle on clean configuration	10

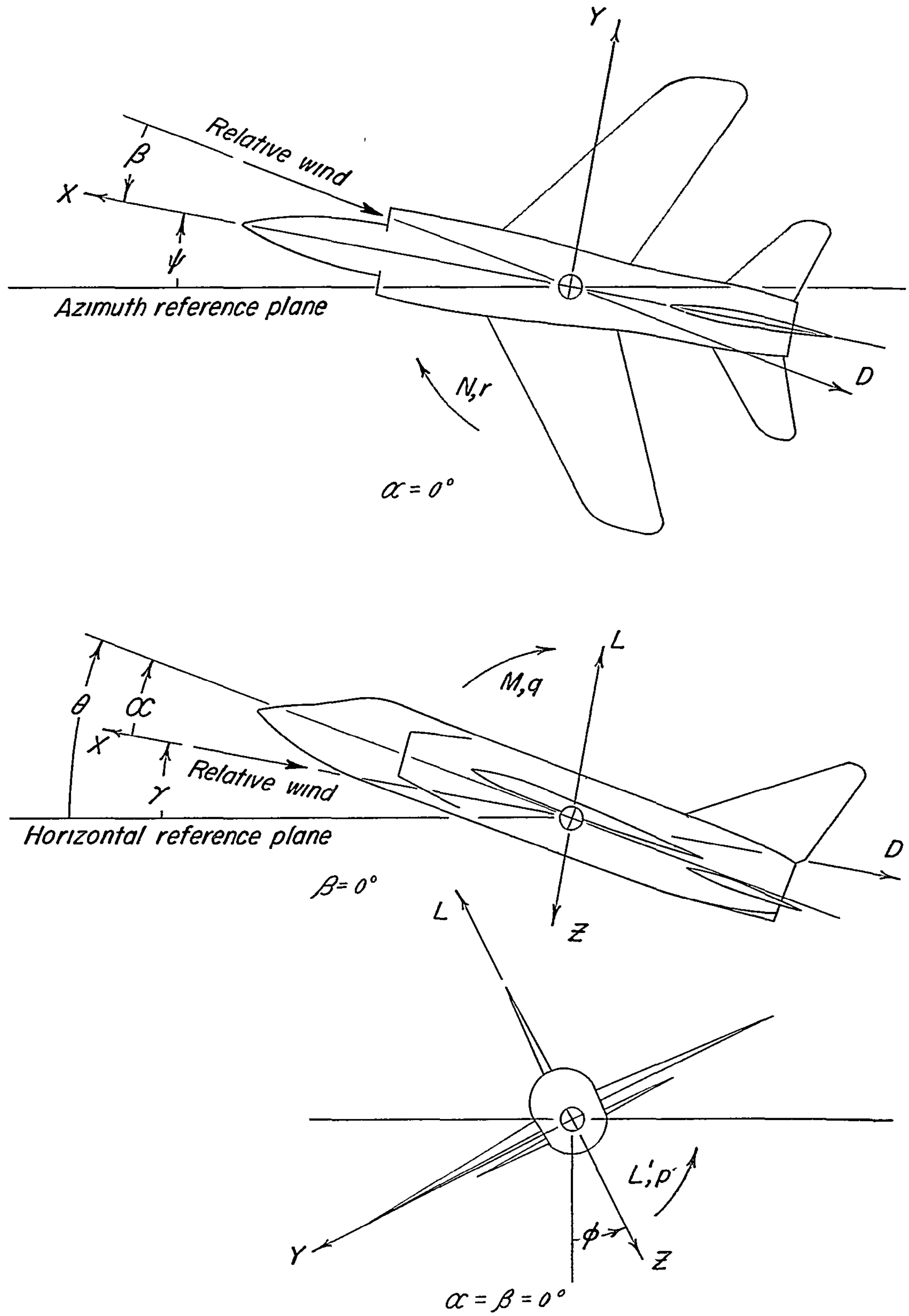

Figure 1.- Stability system of axes. Arrows indicate positive direction of forces, moments, angular displacements, and angular velocities.

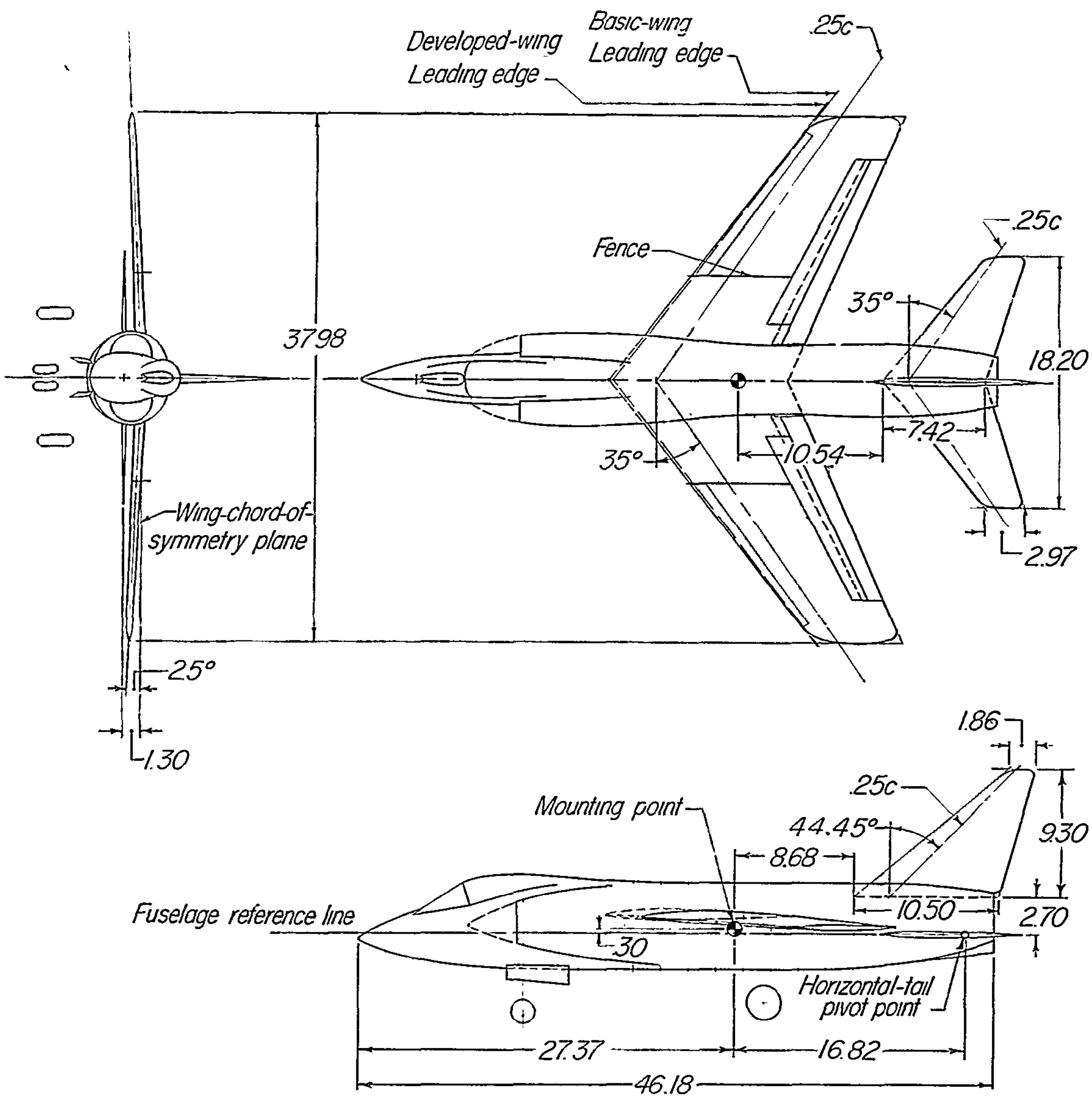

(a) General arrangement.

Figure 2.- Geometric characteristics of 1/10-scale model of the Grumman F9F-9 airplane. All dimensions in inches. All wing dimensions refer to basic wing.

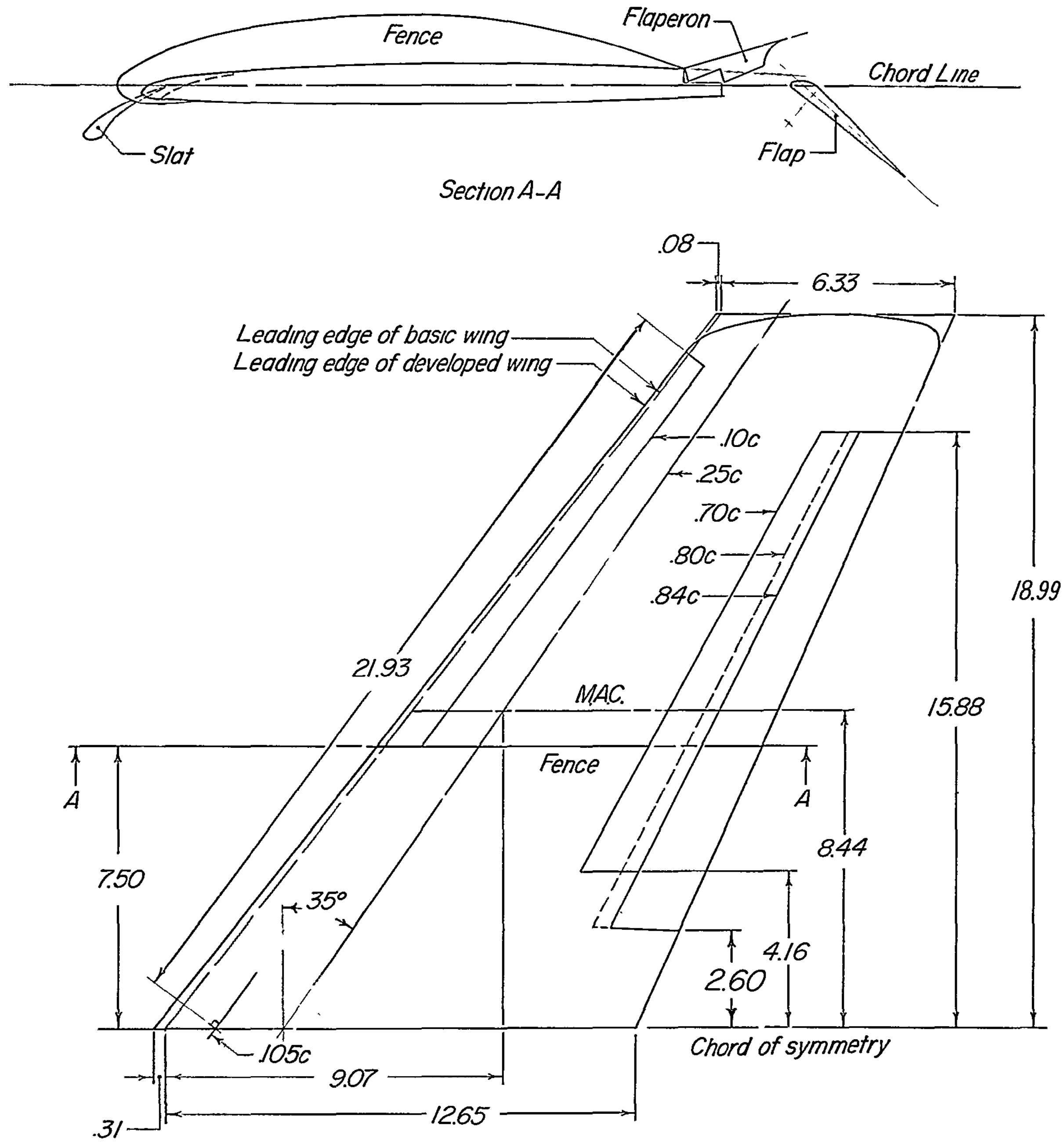

(b) Details of fence, slat, flaps, and flaperon.

Figure 2.- Concluded.

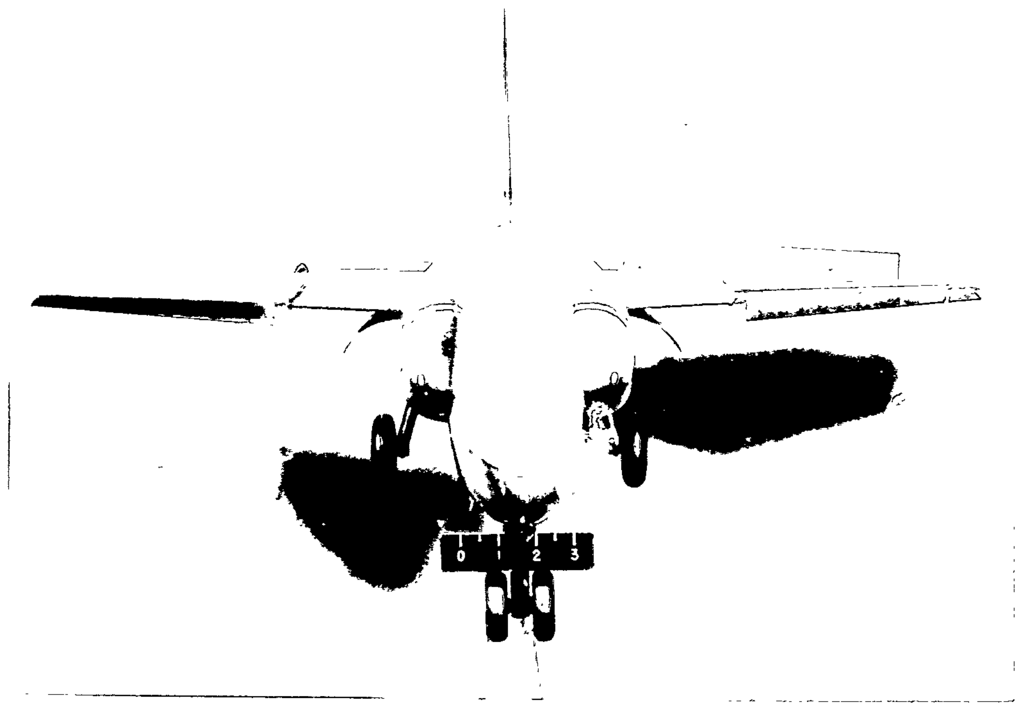

L-87748

(a) Front view of WBZPVH$_{-10}$F$_{30}$S$\delta_L^{55}\delta_R^{5}$G landing configuration.

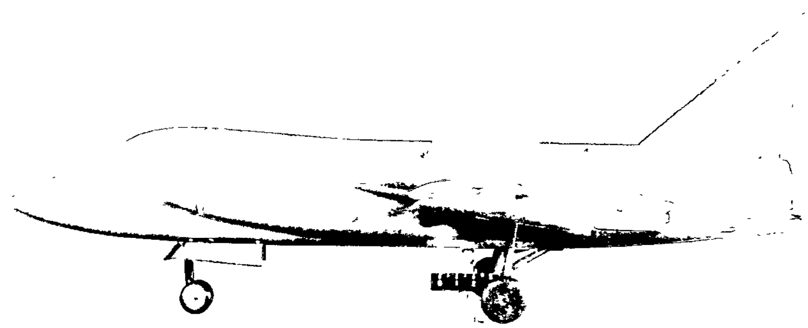

L-87749

(b) Side view of WBZVH$_{-10}$F$_{30}$S$\delta_L^{55}\delta_R^{5}$G landing configuration.

Figure 3.- Photographs of 1/10-scale model of the Grumman F9F-9 airplane mounted on model-support pedestal.

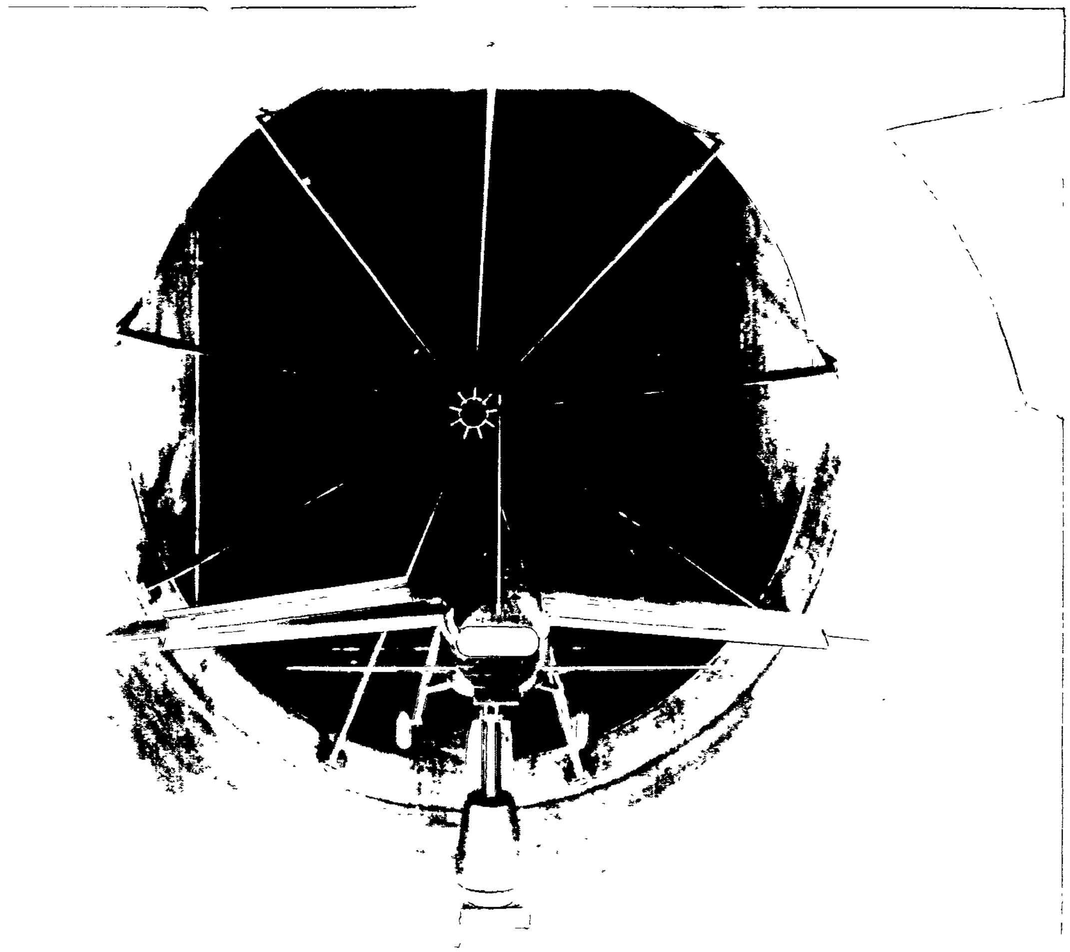

L-87654

Figure 4.- Photograph of 1/10-scale model of the Grumman F9F-9 airplane mounted in the rolling-flow test section of the Langley stability tunnel. $WBZPVH_{-10}F_{30}S\delta_L^{55}\delta_R^{5}G$ landing configuration.

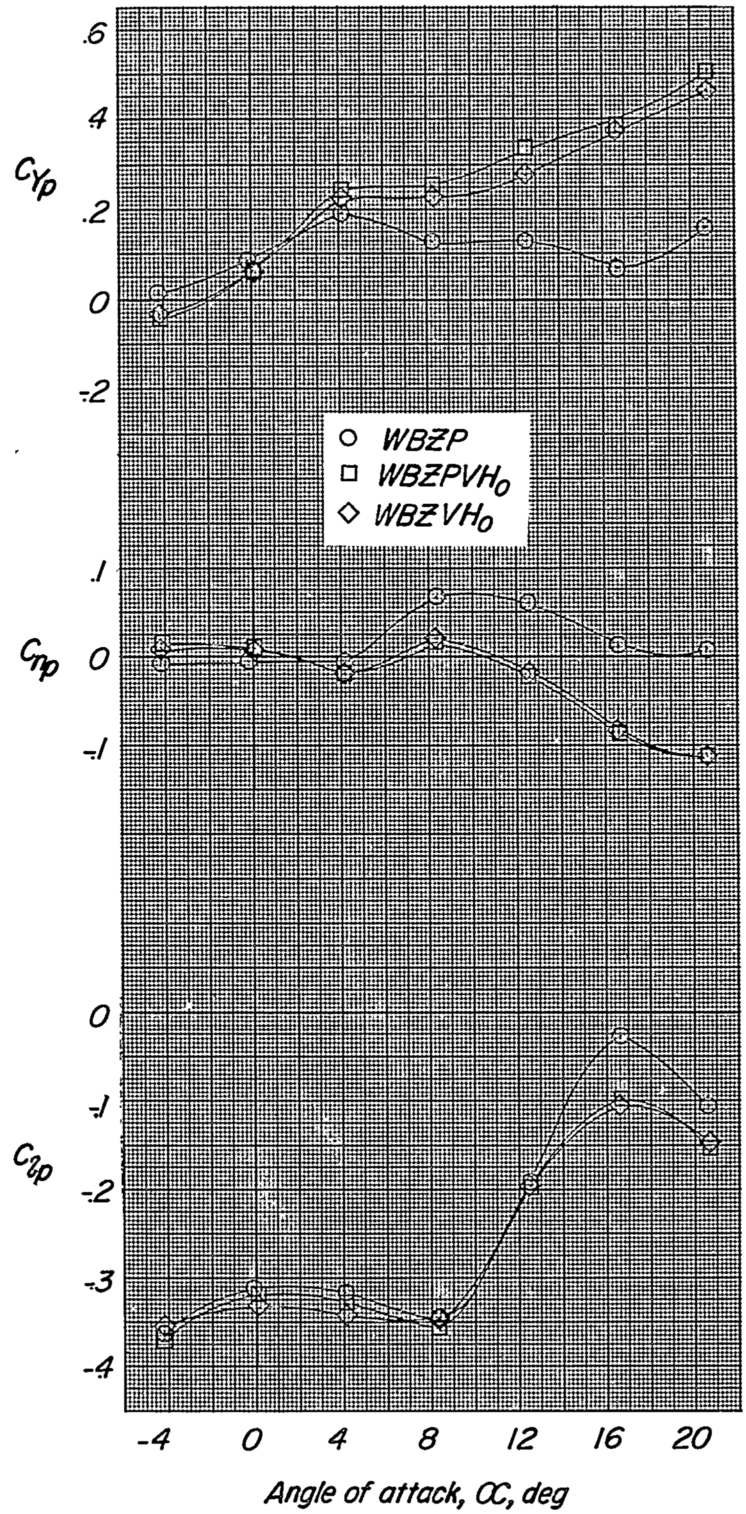

Figure 5.- Effect of horizontal and vertical tails and duct-entrance fairing plugs on the rolling stability derivatives. Slats, flaps, flaperons, and landing gear retracted.

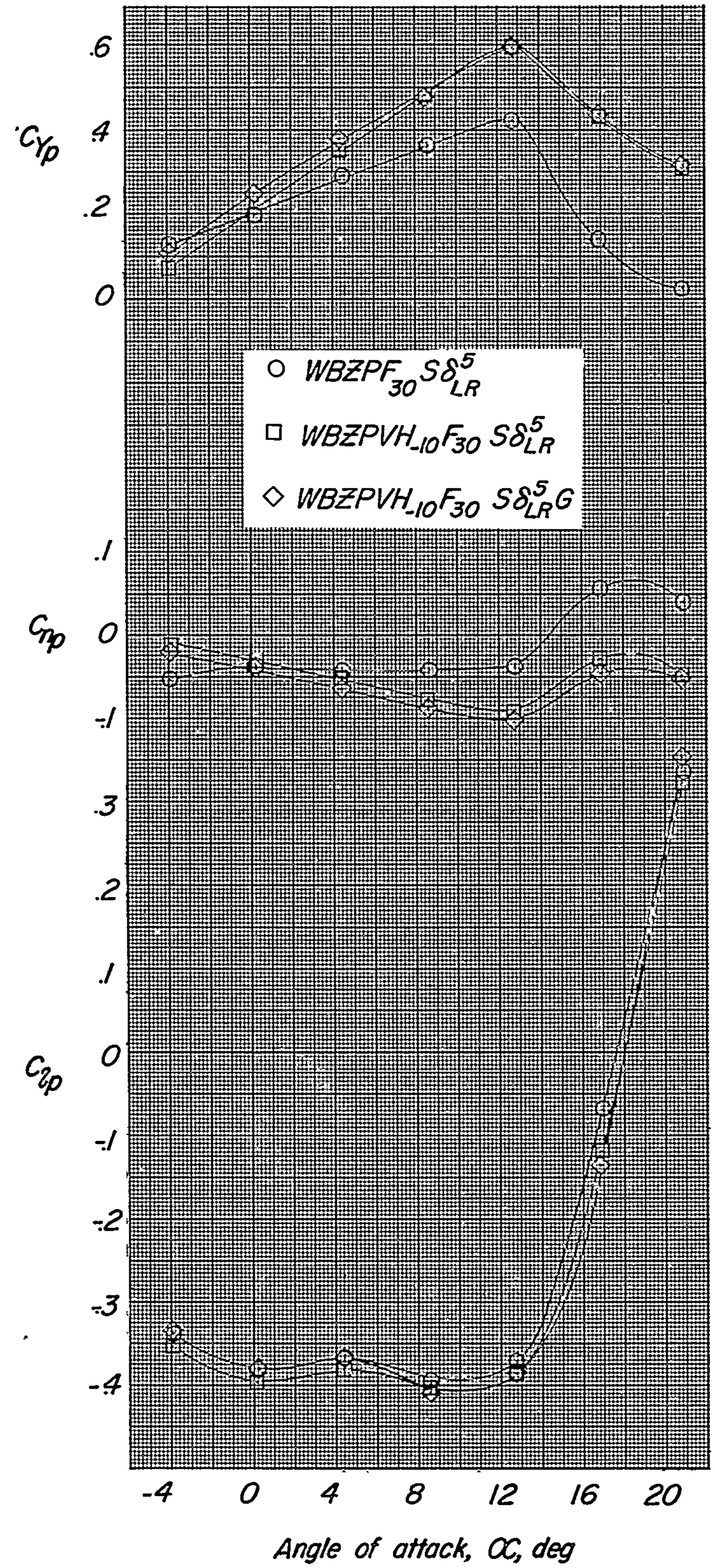

Figure 6.- Effect of horizontal and vertical tails and landing gear on the rolling stability derivatives. Slats, flaps, and flaperons extended.

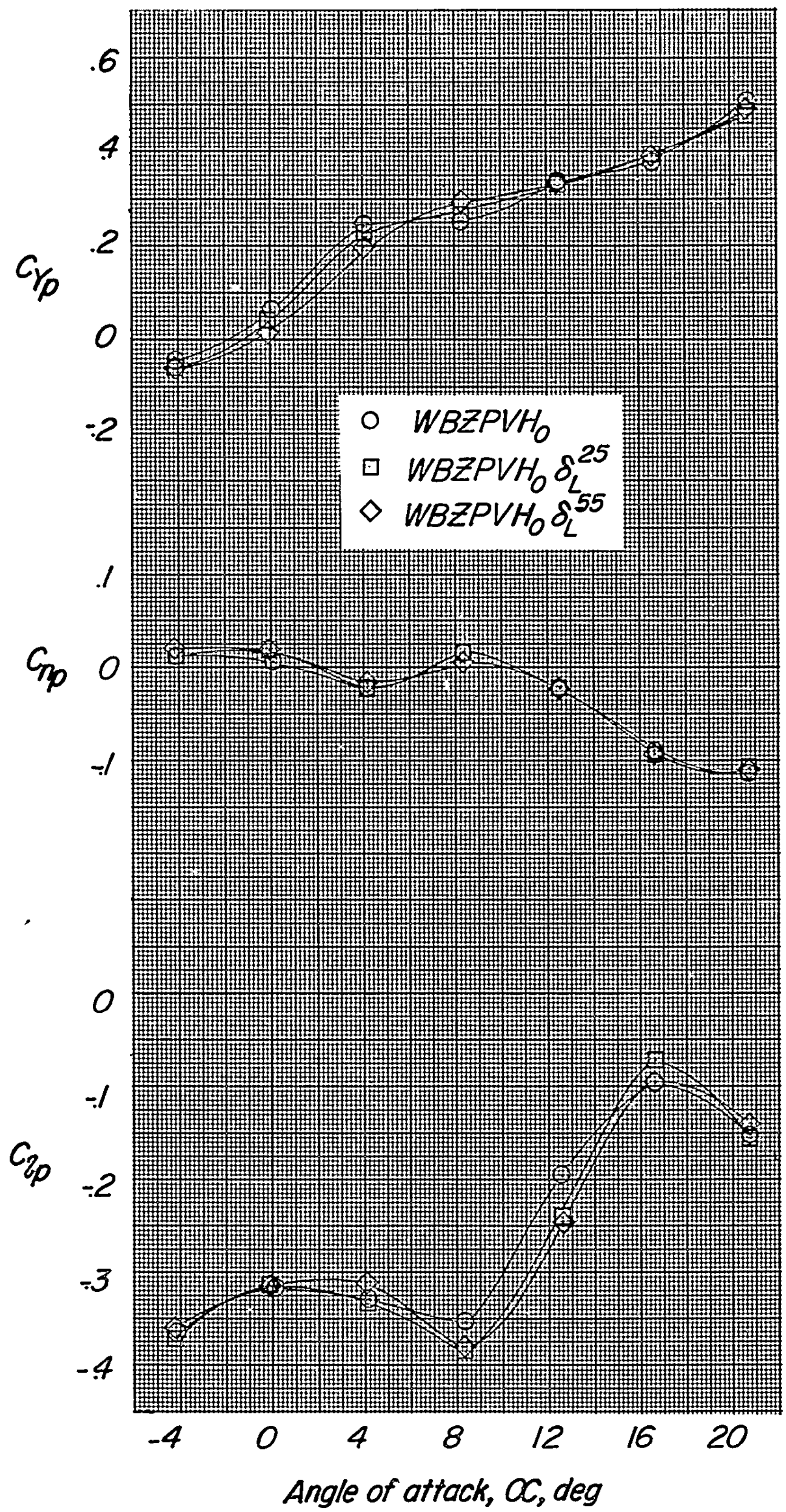

Figure 7.- Effect of flaperon deflection on the rolling stability derivatives. Slats, flaps, and landing gear retracted.

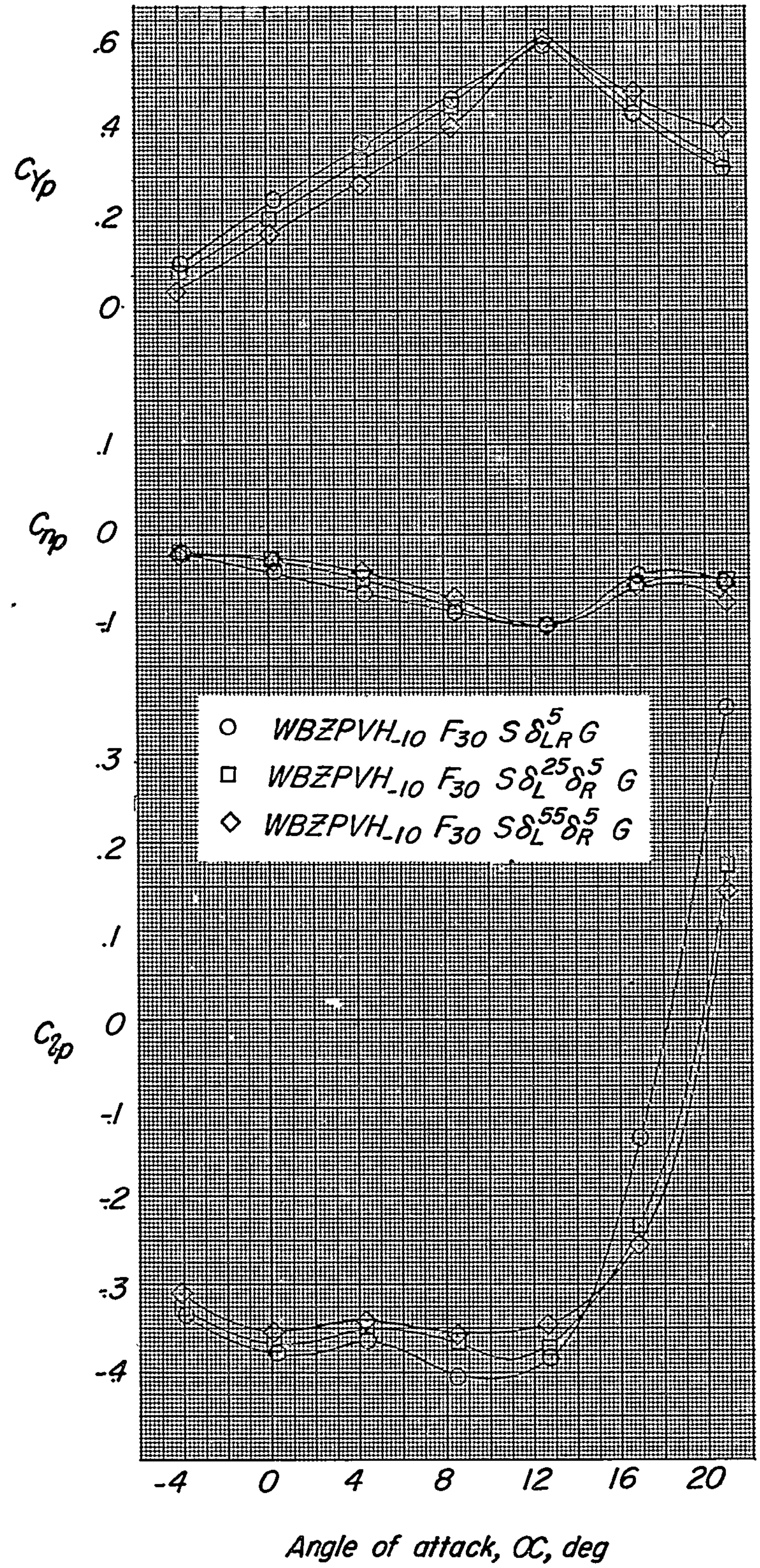

Figure 8.- Effect of flaperon deflection on the rolling stability derivatives. Slats, flaps, and landing gear extended.

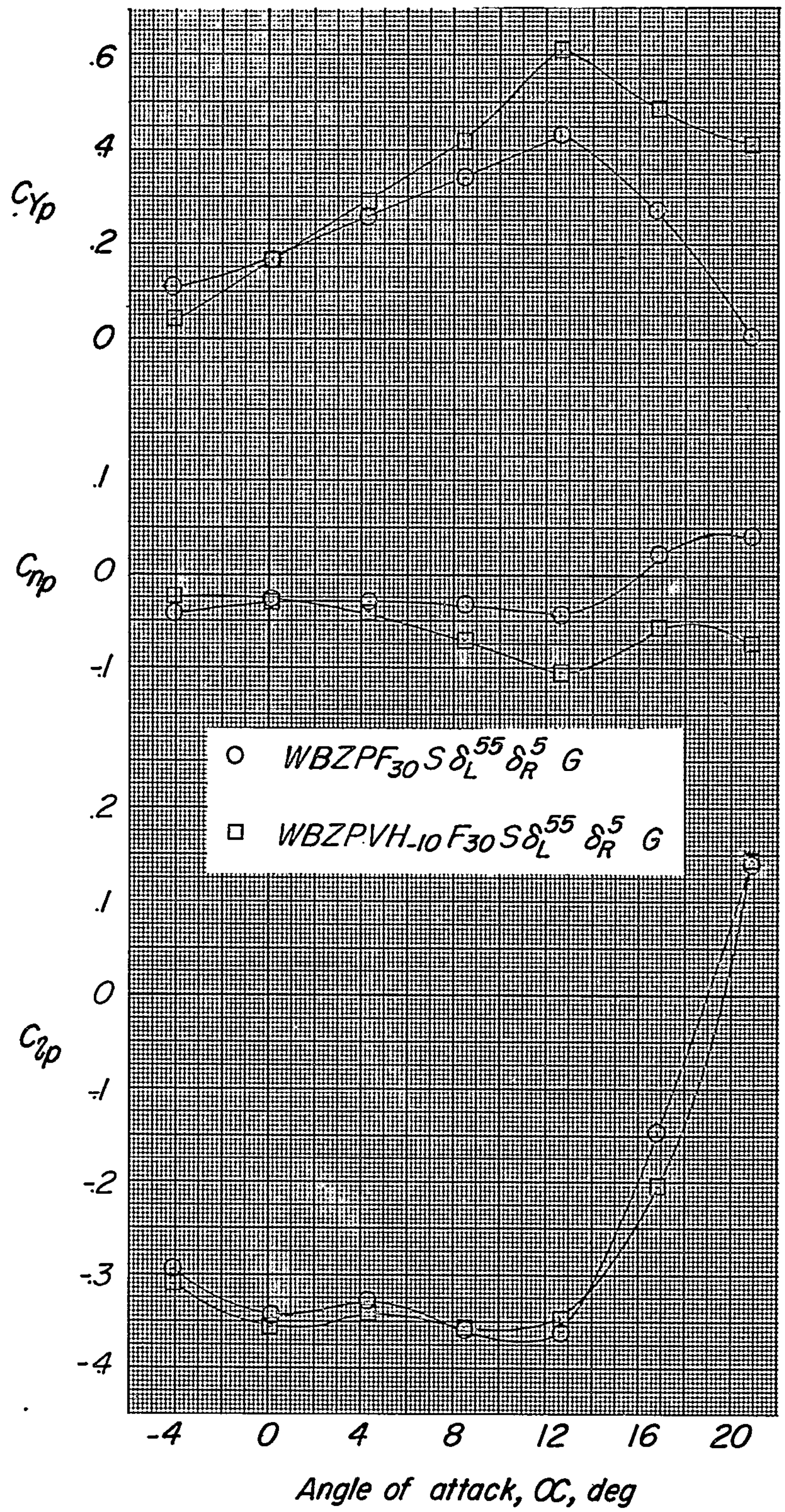

Figure 9.- Effect of horizontal and vertical tails on the rolling stability derivatives. Slats, flaps, and landing gear extended.

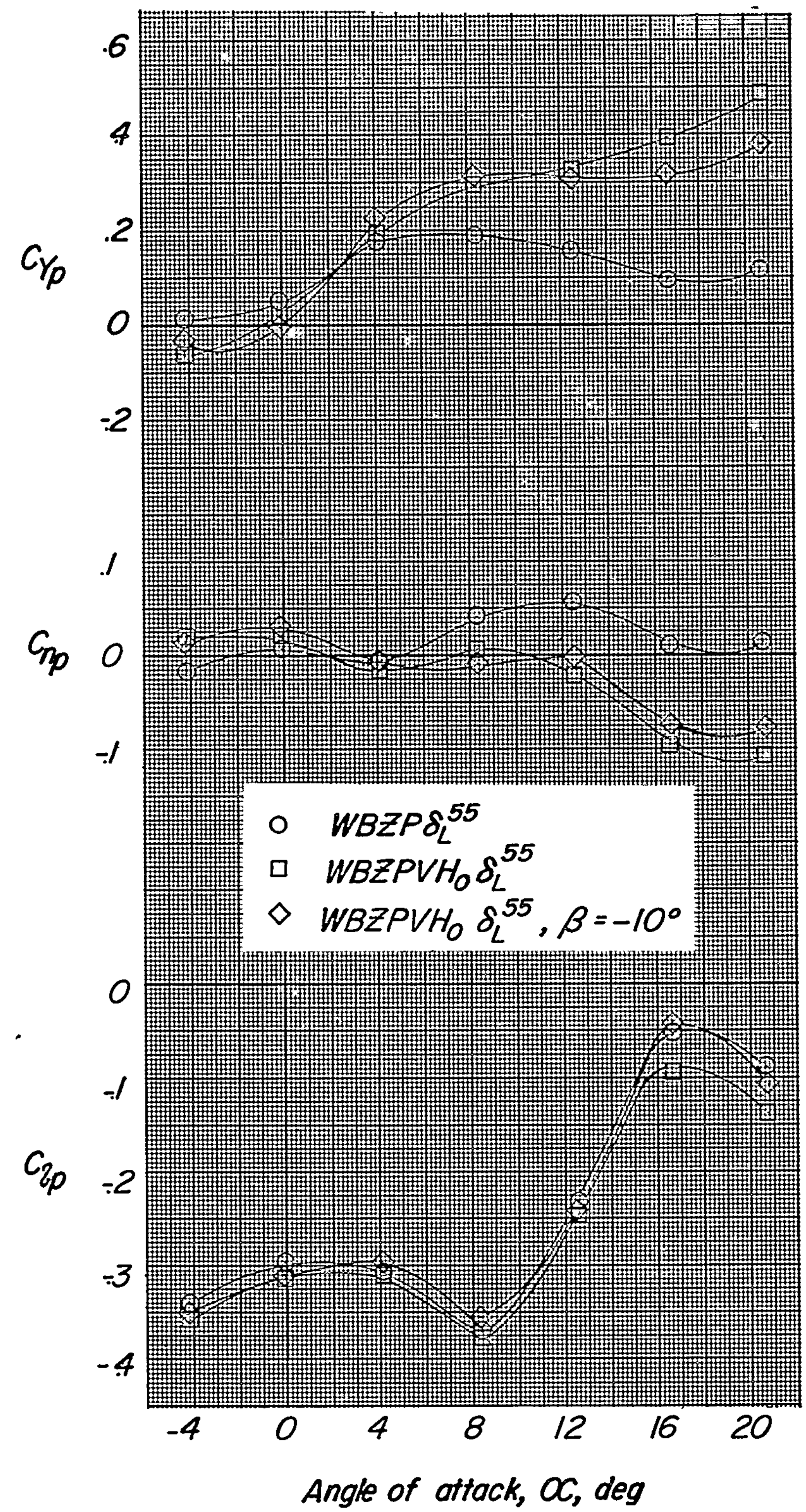

Figure 10.- Effect of horizontal and vertical tails and sideslip angle on the rolling stability derivatives. Slats, flaps, and landing gear retracted.

[redacted]

[redacted]